

THE SEARCH FOR H^- IN ASTROPHYSICAL ENVIRONMENTS

TERESA ROSS,¹ EMILY J. BAKER,^{1,2} THEODORE P. SNOW,¹ JOSHUA D. DESTREE,¹ BRIAN L. RACHFORD,³
MEREDITH M. DROSBACK,¹ AND ADAM G. JENSEN⁴

Received 2008 March 5; accepted 2008 May 21

ABSTRACT

The negative ion H^- is widely understood to be important in many astrophysical environments, including the atmospheres of late-type stars like the Sun. However, the ion has never been detected spectroscopically outside the laboratory. A search for the far-ultraviolet autodetaching transitions of H^- in interstellar and circumstellar matter seems to be the best hope for directly detecting this ion. We undertook a highly sensitive search using data from the *FUSE* instrument. We concentrated on two types of sight lines: planetary nebulae, where model calculations suggest a sufficient abundance of H^- to be determined, and translucent clouds, where H^- might form on dust grains as an intermediate step in molecular hydrogen formation. Upper limits on H^- abundances were set.

Subject headings: ISM: abundances — ISM: atoms — ISM: lines and bands — planetary nebulae: general

1. INTRODUCTION

The search for the elusive H^- ion has been a problem for several generations of astronomers. A host of research in the mid-20th century cemented the place of H^- as the major source of opacity for stars solar-type and later in standard stellar models. Although there has been some IR data that are consistent with the existence of H^- in stellar atmospheres, there has never been a direct detection of H^- in any astrophysical environment. Theory predicts a series of narrow resonances in the UV, which have been measured experimentally in the lab. We have attempted to directly detect these resonances by examining archival *FUSE* data on the most likely sight lines for detection.

1.1. History

By the late 1930s, the astrophysical community had yet to derive a satisfactory model for continuous absorption in the solar atmosphere. It was understood that at photospheric temperatures for late-type stars, little hydrogen would be ionized, which would indicate that the metals must be responsible for absorption. However, if this were the case, it would be expected that there would be observable discontinuities due to the absorption edges of these elements. No such absorption edges have been seen, except for hydrogen and the negative ion of oxygen. In general, the wavelength dependence of the continuous absorption coefficient derived from a model of metal absorption did not describe the observed features of the solar continuum. It was Wildt (1939) who first proposed the inclusion of the H^- in photospheric models to explain observed spectra. The opacity of H^- due to bound-free and free-free absorption was explored throughout the following decade (Chandrasekhar 1944). A paper by Chandrasekhar & Breen (1946) calculated the cross section for free-free absorption, to reasonable accuracy. The cross sections, calculated through quan-

tum mechanics, agreed with values of the absorption coefficient in the Sun derived empirically by Münch (1945). This correlation resulted in the firm acceptance of H^- as the major opacity source in the Sun. It could be assumed that other late-type stars, physically similar to the Sun, must also rely on the negative ion of hydrogen to provide opacity. However, H^- has never been directly detected through signature photoabsorption features.

1.2. The Spectrum of H^-

The spectrum of H^- is largely featureless through the visible and IR spectrum. The bound-free continuum has a threshold at 1.65 μm , and peaks broadly at about 0.8 μm . Longward of 1.65 μm , free-free transitions dominate, and the cross section increases slowly with wavelength.

Features arise, however, in the UV. Within the continuum is a resonance region of doubly excited autodetaching singlet P states. These states correspond to excited states of neutral hydrogen with an extra bound electron. The theoretical existence of these narrow resonances was explored in a series of papers on the scattering of low-energy electrons by neutral hydrogen. Taylor & Burke (1967), in calculating cross sections of scattering, first predicted the location of a singlet P shape resonance. Macek (1967) was the first to calculate the absorption coefficient for the resonance and estimate the strength of the line. This theoretically predicted resonance was first reported to be observed by electron scattering in the laboratory by McGowan et al. (1969). Further theoretical calculations in the mid-70s (Broad & Reinhardt 1976; Lin 1975) predicted the narrow Feshbach resonances redward of the shape, and higher energy resonances.⁵ All resonances have the asymmetric Fano profile typical of autoionizing states. Much laboratory work has gone into refining the values of the wavelengths and line widths of these resonances (Cohen & Bryant 2000; Tang et al. 1994; Balling et al. 2000). While there is still disagreement on the exact positions of the resonances the answers from theory and experiment are getting closer and closer to agreement. The f -values and line widths are listed in Table 1 for the shape resonance and Table 2 for the Feshbach resonance.

¹ Center for Astrophysics and Space Astronomy, Department of Astrophysical and Planetary Sciences, University of Colorado at Boulder, Campus Box 389, Boulder, CO 80309-0391; teresa.ross@colorado.edu, tsnow@casa.colorado.edu, destree@casa.colorado.edu, meredith.droback@colorado.edu.

² Current address: Space Science Institute, 4750 Walnut Street, Suite 205, Boulder, CO 80301; emily.j.baker@colorado.edu.

³ Department of Physics, Embry-Riddle Aeronautical University, 3700 Willow Creek Road, Prescott, AZ 86301; rachf7ac@erau.edu.

⁴ NASA Postdoctoral Program Fellow, NASA Goddard Space Flight Center, Code 665, Greenbelt, MD 20771; adam.g.jensen@nasa.gov.

⁵ In recent years much more work has been done to explore resonances at higher n states (Modeley et al. 2003; Chen 2002). Dozens of other resonances have been identified but are not used in this study.

TABLE 1
PROPERTIES OF H⁻ SHAPE ABSORPTION FEATURES

Wavelength (Å)	<i>f</i> -Value	Γ (Line Width) (Å)	Reference
1129.96 ± 0.07....	0.0178 ^a	2.2	Cohen & Bryant (2000)
1131.66.....	Balling et al. (2000)
1130.55.....	...	4.49	Tang et al. (1994)
1130.10 ^b	0.024 (±15%)	1.55	Broad & Reinhardt (1976)
1129.54.....	0.044	1.55	Macek (1967)

^a Estimated by multiplying area under the curve by $(4\pi^2\alpha a_0^2)^{-1}$, the same technique used by Macek (1967).

^b The transition wavelength is the two-electron binding energy converted from a.u. to energy with respect to the ground state; 1 au = 27.2113962M/(M + m) eV and the ground-state energy of H⁻ = 14.35265 eV.

1.3. Previous Attempts at Direct Detection

The possibility that interstellar H⁻ had been detected was raised when Rudkjøbing (1969) suggested that the negative ion might be responsible for four of the unidentified diffuse interstellar bands (DIBs). Rudkjøbing's reasoning was based on an extrapolation from an isoelectronic sequence. He argued since these four bands, at 4430, 4760, 4890, and 6810 Å, were broader than other DIBs, they must come from the same source. In Rudkjøbing's model, the breadth of the lines could be explained by the short lifetimes of the upper states of transitions in H⁻. This theory was discounted in a paper by Snow (1973), who pointed out that this theory relied on singly excited states of H⁻, which do not exist. In general, there is no theoretical or experimental evidence to suggest that H⁻ is capable of producing absorption features such as the DIBs. Also, were such features caused by H⁻ it would be expected that their abundance in the solar photosphere would cause them to be seen in the visible spectrum of the Sun.

Some hope for direct detection arose in the mid-1960s when the data obtained from the balloon-borne IR spectrometer Stratoscope II showed a peak at 1.65 μm for spectra of several stars (Woolf et al. 1964). This feature is exactly what one would expect for a stellar atmosphere dominated by H⁻, as it occurs at the minimum of the ion's absorption coefficient, between the bound-free and free-free absorption. This feature was confirmed in ground-based observations by Bahng (1969). Further observational evidence pointing to the existence of H⁻ was seen in the IR excess of Be stars as explored by Schild et al. (1974). They concluded that a broad peak seen at 1 μm was consistent with H⁻ free-bound emission in a thin circumstellar shell. Schild's findings indicated a column density of about 10¹⁵ cm⁻² for H⁻, making Be stars good candidates for detection of the predicted UV resonance.

Based on Schild's prediction Snow (1975) made an attempt to detect H⁻ in the UV. The theoretical predictions of Macek were

used as a guide. Observations were made with the Copernicus instrument, with little success. The data indicated an upper limit of 2×10^{14} cm⁻², casting doubt on either the conclusions about the source of the IR emission, the theoretical predictions of the resonance, or the appropriateness of Be stars for this type of study.

Andre et al. (2002) presented a poster on their attempts to detect H⁻ in the interstellar medium. They surveyed lines of sight to several early-type stars, but did not see any H⁻ absorption.

With new laboratory measurements of H⁻ resonances and the enhanced far-UV sensitivity of *FUSE*, now seems to be a good time to resurrect the search for H⁻. After a brief discussion of the physics of the ion, this paper will examine the environments most likely to have a significant H⁻ abundance. A discussion of the data quality, analysis, and characteristics adding to the difficulty of observing these resonances will follow.

2. PHYSICS OF H⁻ ION

The H⁻ ion forms due to the large polarizability of the neutral hydrogen atom. In the limit of a free electron approaching a neutral hydrogen atom from a large distance the electron will induce a dipole moment in the atom leading to a quasi-bound state. This interaction leads to the continuous absorption that is the main contributor to the opacity of cool stars. The two processes by which the ion interacts with the radiation field are (Mihalas 1978) the bound-free

$$\text{H}^- + h\nu \Leftrightarrow \text{H} + e(\nu) \quad (1)$$

and free-free

$$\text{H} + e(\nu) + h\nu \Leftrightarrow \text{H} + e(\nu'). \quad (2)$$

For the H⁻ ion the electron-electron interactions are as important as the interactions between the electrons and the nucleus.

TABLE 2
PROPERTIES OF H⁻ FESHBACH ABSORPTION FEATURES

Series Number	Wavelength (Å)	<i>f</i> -Value	Γ (Line Width) (mÅ)	Reference
1.....	1134.93	1.28×10^{-3a}	5.9	Balling et al. (2000) ^b
	1134.97	...	6.1	Tang et al. (1994)
	1134.82 ^c	Broad & Reinhardt (1976)
2.....	1132.08	5.46×10^{-5a}	0.4	Balling et al. (2000)
	1132.07	Tang et al. (1994)

^a Estimated by multiplying area under the curve by $(4\pi^2\alpha a_0^2)^{-1}$, the same technique used by Macek (1967).

^b See chart of Feshbach resonances in this paper and citations therein for more theoretical and experimental values.

^c Same conversion as shape resonance above.

This prevents us from neglecting electron correlation, and the usual Hartree-Fock variational approach with each electron seeing an effective potential due to shielding from all the other electrons, is generally inadequate. The overall cross-section for interaction due to bound-free and free-free emission was determined by Chandrasekhar & Breen (1946). They used a Hartree-Fock-type method, but introduced a more sophisticated wave function, allowing two different shielding factors, suggesting a situation where one electron is much closer to the nucleus than the other.

Since then, the theoretical calculations of the cross section of H^- have become more precise, thanks to a number of clever quantum mechanical techniques. Today, H^- is most often described in hyperspherical coordinates, which incorporate the electron correlation from the first. In this formality, resonances occur when the hyperradius [$R \equiv (r_1^2 + r_2^2)^{1/2}$, where r_1 and r_2 are the radii of the two electrons] is finite and the electrons are “bound” to the nucleus in a slowly varying hyperspherical potential. As R gets large, these potentials approach the state of an electron bound to a neutral atom in an induced dipole potential.

For a system approaching the neutral-atom threshold with principle quantum number n , the dipole states are given by $m = n + 1, n + 2, \dots$, and so on. The lowest resonance in a given potential is given $m = n$. In this state, the two electrons are a comparable distance from the nucleus, and thus interact very strongly, making this a very unstable state and quick to autodetach. Increasing m gives states where one electron is increasingly far away from the nucleus, reducing interelectron interactions except through the dipole moment. Thus, states with higher m are more stable. In the spectrum, this results in a series of resonances that decrease in width as they increase in energy. Such series theoretically exist below the threshold for each excited state of neutral hydrogen. They have been experimentally measured below $n = 2$ (Bryant et al. 1977; Cohen & Bryant 2000; Balling et al. 2000) and $n = 3$ (Modeley et al. 2003). (Much of the information in this section was gleaned from Balling et al. 2000 and Rau 1996.)

2.1. Fano Profile

The independent electron approximation breaks down in cases of double-excited atoms and autoionizing states, both relevant to the study of H^- ion. By including the electron correlations which become important in these cases, it becomes necessary to describe electron configurations as superpositions of stationary states. The resonances of H^- lie in the continuum, which means their natural line shape will be determined by the mixing of a discrete electron configuration and a continuum of electron states. Fano (1961) developed a theoretical formula for the line shape resulting from autoionizing transitions, aptly known as the Fano profile which appears as follows:

$$\sigma(E) = \sigma_a \frac{[q + \epsilon(E)]^2}{1 + \epsilon(E)^2} + \sigma_b, \quad (3)$$

where q is a parameter describing the asymmetry, σ_a is a scaling factor, σ_b is an offset, and $\epsilon(E)$ is given by

$$\epsilon(E) = \frac{E - E_0}{\Gamma/2}. \quad (4)$$

Here, Γ is the spectral line width and E_0 is the energy of line center.

2.2. Laboratory Experiments

The basic scheme of experiments to measure the resonances of H^- involves colliding a beam of the ions with something that will cause them to detach, then counting what percentage of the atoms are neutralized. The first detection of the shape resonance was

achieved by electron scattering experiments (McGowan et al. 1969). However, more precise measurement of the shape resonance and the next highest Feshbach resonance was done with the “colliding beam method” pioneered by a group at Los Alamos (Bryant et al. 1977). These experiments shot bursts of nitrogen laser light through an accelerated beam of H^- ions. After each pulse, the photodetached electrons were magnetically deflected from the beam into a solid state detector. This method was improved on by Balling et al. (2000) with the use of vacuum ultraviolet (VUV) laser technology, which improves the resolution.

3. CHOICE OF SIGHT LINE

A study by Black (1978) examined the existence and balance of molecules in the transition zones of ionized nebulae. The goal of the model was to match observed data of NGC 7027 to better understand the relevant chemistry. Such regions are likely to include both neutral hydrogen and free electrons, which make the existence of H^- quite likely. Black’s models included the formation of H^- , its destruction through associative detachment to form H_2 , photodetachment, and mutual neutralization with an arbitrary positive ion. This model predicted the density of H^- in the transition zone of planetary nebulae to range from 1×10^{-5} to $1 \times 10^{-4} \text{ cm}^{-3}$. Integrated over the transition zone, there is a column of $3.5 \times 10^{12} \text{ cm}^{-2}$. Compared to Be stars, the geometry of planetary nebulae is less complex, and it is unlikely that H^- could exist in “clumps” that do not intersect our line of sight, nor do we expect variable emission. Thus, planetary nebulae are likely candidates to observe H^- resonances. Of course each planetary nebula is different so this predicted H^- column density is only an order of magnitude estimation, not a predicted column density for each planetary nebula.

Other astrophysical environments where H^- could be detectable are in photodissociation regions and dark clouds. A recently proposed model (Field 2000) of molecular hydrogen formation on dust grains presents H^- as an intermediate step, indicating that an observable amount of the negative ion could exist. Field hypothesizes that H^- may be produced efficiently on the surface of dust grains, followed by creation of H_2 via gas phase associative detachment. Field goes on to assume that his theoretical dust grains bind electrons to their surface with an energy less than the binding energy of hydrogen to the surface subtracted from the electron affinity of neutral H. He then calculates the rate coefficients for the formation and destruction of H^- and assumes a steady state to estimate abundances. Field (2000) states the predicted H^- number density is given by the equation:

$$n(H^-) = \frac{kn(H_{\text{total}})n(H)}{k^{(-)}n(H) + k^{\text{ph}} + k^{(+)}n(I^+) + k^{\text{add}}}, \quad (5)$$

where $n(H_{\text{total}}) = n(H) + 2n(H_2)$, $n(H)$ is the number density of H I, and $k \sim 6.6 \times 10^{-18} T^{1/2} \text{ cm}^3 \text{ s}^{-1}$ the second-order rate coefficient for H_2 formation. In the denominator the first term, $k^{(-)}$ ($= 1.3 \times 10^{-9} \text{ cm}^3 \text{ s}^{-1}$), is the rate coefficient for the reaction of H with H^- (Schmeltekopf et al. 1967). In the unshielded ISM, Rawlings et al. (1988) give the rate for photodetachment integrated over all wavelengths as $k^{\text{ph}} \sim 3.4 \times 10^{-8} \text{ s}^{-1}$. The rate coefficient $k^{(+)} = 4 \times 10^{-6} T^{-1/2} \text{ cm}^3 \text{ s}^{-1}$ is the rate of H^- removal through reaction with all positive ion species $n(I^+)$ (Dalgarno & McCray 1973); k^{add} encompasses other H^- destruction processes but is found to be negligible (Field 2000).

Using equation (5) and standard numbers for the ISM, such as $n \simeq 100 \text{ cm}^{-3}$, $T \simeq 150 \text{ K}$, and $n(I^+) \simeq 10^{-4} \text{ cm}^{-3}$, we have estimated the number density of H^- for particular sight lines. Furthermore we estimated the column density $N(H^-)$ for seven

TABLE 3
OBSERVATIONAL PARAMETERS FOR *FUSE* TARGETS

Target	Sight-Line Type	S/N	$E(B - V)$	$\log N(H\ I)$ (cm^{-2})	Fraction H_2	Reference ^a	Estimated $\log N(H^-)$ (cm^{-2})	Reference ^b	2σ Upper Limit $\log N(H^-)$ (cm^{-2})
HD 216532	Reddened O8.5 V	19.9	0.85	15.80
HD 217035AB	Reddened B0 V	12.4	0.76	21.46 ± 0.12	...	1	14.1	2	16.00
HD 23625	Reddened B2.5 V	38.4	0.56	15.52
HD 99872	Reddened B3 V	32.0	0.42	15.60
HD 144965	Reddened B3 Vne	37.4	0.45	15.53
IC 2448	Planetary nebula	26.4	12.5	3	15.68
NGC 5882	Planetary nebula	11.8	12.5	3	16.03
WD 0439+466	Planetary nebula	30.0	12.5	3	15.62
HD 039659	Planetary nebula	21.7	12.5	3	15.76
HD 110432	Translucent cloud	44.1	0.40	20.85 ± 0.15	0.55	4	12.6	2	15.46
HD 185418	Translucent cloud	36.0	0.51	21.11 ± 0.15	0.47	4	13.5	2	15.54
HD 197512	Translucent cloud	17.4	0.33	21.26 ± 0.15	0.33	4	14.0	2	15.86
HD 199579	Translucent cloud	49.7	0.36	21.04 ± 0.11	0.38	4	13.7	2	15.40
HD 207198	Translucent cloud	25.3	0.62	21.34 ± 0.17	0.38	4	14.0	2	15.70
HD 210893	Translucent cloud	56.3	0.56	21.15 ± 0.10	0.49	4	13.1	2	15.35

^a References for $H\ I$ column densities: (1) Diplás & Savage (1994); (4) Rachford et al. (2002).

^b Predicted column densities of H^- : (2) Calculated with eq. (5); (3) based on planetary nebulae model by Black (1978).

sight lines by using the fraction of $n(H^-)/n(H_{\text{tot}})$ multiplied by the measured $N(H_{\text{tot}})$ along the line of sight. The $N(H^-)$ abundance estimates, reported in Table 3, range from 4.0×10^{12} to $1.3 \times 10^{14} \text{ cm}^{-2}$.

4. MODELING

To get an idea of what the H^- features look like, a model was created (Fig. 1). The model plotted the absorptions for column

densities of 10^{13} , 10^{14} , and 10^{15} cm^{-2} from the shape and two Feshbach resonances on a flat continuum of one. Thus the model is the percentage of absorption expected, and was scaled to overlay on the spectroscopic data of HD 110432.

The shape resonance was modeled with a Fano profile (eq. [3]) using the line parameters reported in Table 4. The Feshbach resonances naturally have Fano profiles also, but were modeled with Gaussians since the instrumental resolution of *FUSE* smears out

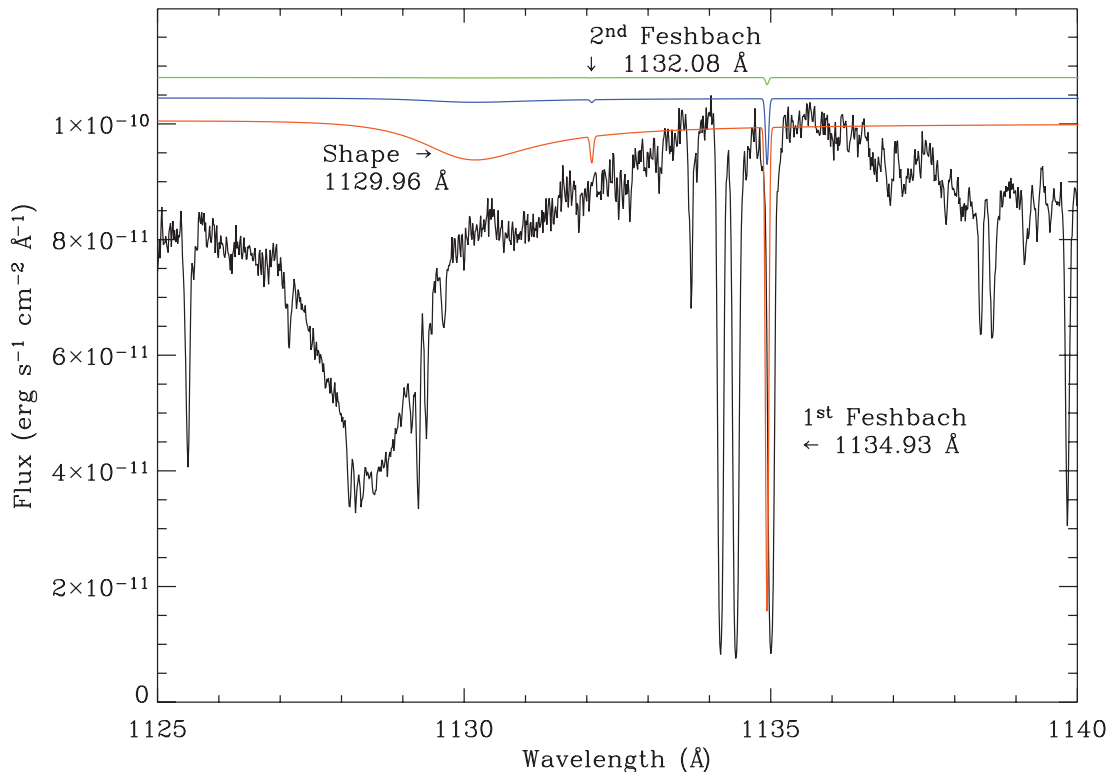


FIG. 1.— Each colored line shows the expected absorption by H^- for column densities of 10^{13} cm^{-2} (green), 10^{14} cm^{-2} (blue), and 10^{15} cm^{-2} (red) scaled to be shown near the continuum flux level of HD 110432. The absorption models include the H^- shape and two Feshbach resonances.

TABLE 4
PARAMETERS USED TO GENERATE
THE SHAPE RESONANCE FANO PROFILE

Parameter	Shape ^a (1129.96 Å)
Energy pole.....	10.9724 eV
Γ	21.2 meV
q	-4.92
σ_a	$5.94 \times 10^{-19} \text{ cm}^2$
σ_b	$9.31 \times 10^{-18} \text{ cm}^2$

^a Values taken from Cohen & Bryant (2000).

the extremely narrow intrinsic profile. The parameters used to make the Gaussian features are reported in Table 2.

Oscillator strengths were needed to make the Gaussian features, but were scarce in the literature. To get the f -values we utilized the technique Macek (1967) used to find the shape resonance f -value. He found the f -value by multiplying the area under the photo-absorption cross section curve by $(4\pi^2 \alpha a_0^2)^{-1}$. Lindroth (1995) did experimental lab work and obtained the photodetachment cross section for the H^- resonances, and reported the integrated areas underneath the peak. The oscillator strength for the first and second Feshbach resonances are $f = 1.28 \times 10^{-3}$ and $f = 5.46 \times 10^{-5}$, respectively.

The 10^{13} cm^{-2} model (Fig. 1, *green line*) shows nearly a straight line, except for the first Feshbach resonance with $W_\lambda \lesssim 0.2 \text{ mÅ}$ over the $N \text{ I}$ feature. A column density less than this is completely undetectable even if the $N \text{ I}$ feature was not there. All the planetary nebula, as well as HD 110432, are predicted to have less abundance than 10^{13} cm^{-2} . The largest estimated H^- column (for HD 217035AB) is $1.3 \times 10^{14} \text{ cm}^{-2}$, just slightly more than the 10^{14} cm^{-2} model (*blue line*); this is also undetectable in the *FUSE* spectra with a $W_\lambda \lesssim 2 \text{ mÅ}$ for the first Feshbach resonance and $\lesssim 0.1 \text{ mÅ}$ for the second. All other estimated abundances fall between these models. The model for a column of 10^{15} cm^{-2} (*red line*) gives us hope that H^- will be detectable along interstellar sight lines should the abundance be near or above this amount. More H^- is expected along denser sight lines where there is more total hydrogen, since H^- is a formation pathway for H_2 .

5. DATA ANALYSIS AND DISCUSSION

All data were taken from the *FUSE* instrument, a UV satellite telescope in low Earth orbit. For specifications on *FUSE* please see Moos et al. (2000). The one detector peculiarity that affected the study was the infamous “worm.” A worm is a dark horizontal or diagonal line appearing in the two-dimensional spectroscopic data, caused by the shadow of grid wires on the MCPs. In the data we obtained, “the worm” appears as a wide band of extinction between 1140 and 1160 Å. The main concern is uncertainty in the continuum for fitting absorption lines, but we are looking shortward of this extinction, and the resonances were not detected, so the worm’s effects are negligible. The other concern is that the worm reduced the signal on the detector enough to make the H^- resonances blend in with the noise.

Public data on planetary nebula and dark cloud sight lines were obtained from the MAST *FUSE* archive. Data on dense PDRs were taken from the *FUSE* translucent cloud survey. The data were calibrated with version 3.1.4 or newer of the CALFUSE pipeline. For each observation we used a cross-correlation analysis to align the individual calibrated exposures using strong absorption features before co-adding the data. Individual detector segments were co-added before measurements were made.

TABLE 5
 $N \text{ I}$ COLUMN DENSITIES

Target (HD)	$\log N(N \text{ I})$ (cm^{-2})
110432.....	$17.09^{+0.19}_{-0.18}$
185418.....	$17.04^{+0.25}_{-0.23}$
197512.....	$16.96^{+0.21}_{-0.19}$
199579.....	17.16 ± 0.10
207198.....	$17.41^{+0.18}_{-0.19}$
210893.....	$17.19^{+0.13}_{-0.12}$

NOTE.—Data from Jensen et al. (2007).

The region around 1130 Å was examined for the shape and two Feshbach resonances; all are singlet P states below $n = 2$. The shape resonance is extremely broad, while the nearby Feshbach series are extremely narrow. Examining the spectra for all three lines revealed no detection of the expected resonances. So, 2σ upper limits were set on the column density using the Jenkins et al. (1973) formula:

$$\epsilon_W = \frac{\Delta \lambda M^{1/2}}{S/N}, \quad (6)$$

where $\Delta \lambda$ is the pixel scale, M is the width of the line (in this case the resolution elements of *FUSE*), and S/N is the signal-to-noise ratio. We could not set upper limits based on each line, due to complications with the spectra. The shape resonance is obscured not only by many $C \text{ I}$ lines but also by prominent stellar features, making the continuum undefinable, disabling the use of this feature to set upper limits. The first Feshbach resonance ($\sim 1134.92 \text{ Å}$) is overshadowed by the nitrogen multiplet (1134.17, 1134.41, 1134.66, and 1134.98 Å). With the strength of these lines there is not much hope for detecting the first Feshbach resonance unless there is very little nitrogen along a line of sight. Table 5 reports $N \text{ I}$ column densities found by Jensen et al. (2007) for the translucent sight lines; in examining the rest of our data, the nitrogen lines are saturated in every sight line, so again we could not set upper limits based on the first Feshbach resonance. The second Feshbach resonance (1132.07 Å) is the only line where Jenkins’ equation is applicable. Thus the upper limits were set with the weakest of the three lines.

Table 3 lists all of our upper limits for the H^- column densities. The H^- column density of $3.5 \times 10^{12} \text{ cm}^{-2}$ indicated by Black’s predictions for planetary nebulae is well below the 2σ upper limits that range from 4.2×10^{15} to $1.1 \times 10^{16} \text{ cm}^{-2}$. With reddened and translucent sight lines the estimates are not as far off from the upper limits. They range from 4.0×10^{12} to $1.3 \times 10^{14} \text{ cm}^{-2}$, but the upper limits are orders of magnitude larger at 2.2×10^{15} to $1.0 \times 10^{16} \text{ cm}^{-2}$, thus inhibiting us from constraining the predictions for H^- . If such column densities were to be detected directly through the observation of UV resonances, an instrument with a sensitivity at least 10 times that of *FUSE* would be necessary. Also an instrument with better spectral resolution would not smear out the Feshbach resonances, allowing the narrower and deeper natural shape of the lines to be seen above the noise.

6. CONCLUSION

With the understanding and current theory on the subject, there can be little doubt that H^- exists in the ISM, yet it still eludes those who would search for it and measure its abundance. The models we created illustrate the difficulty in detecting the H^- features in

spectroscopic data (Fig. 1). There are several reasons to expect the H⁻ resonance features to be hard to find in the ISM. The most obvious is simply that H⁻ is not predicted to exist in any large quantities, making these features weak. All of the predicted column densities were one to several orders of magnitude below the upper limits derived from the *FUSE* spectra.

Second, we have found that the crowded nature of the region would mask the most prominent H⁻ feature if it were present in a measurable amount. The first Feshbach resonance is crowding in on the 1134.98 Å N I feature. There is slight disagreement on the precise wavelength, but the majority of the predictions place the line very close to the N I feature confirming the difficulty in detecting H⁻.

Unfortunately, further searches for astrophysical H⁻ will be difficult—but the problem is very important, given the impact of H⁻ in astrophysics. We have already stressed the role of H⁻ in stellar atmospheric opacities, and we also point out the importance

of H⁻ in the early universe, long before any stars were formed: H⁻ is thought to have been essential to the creation of H₂ in a dust-free environment, and H₂ was necessary for the first stars to be formed (see Glover et al. 2006, and references cited therein). Therefore, further efforts to detect astrophysical H⁻ will be warranted, when the appropriate instruments become available. At this time, there are no plans for future far-UV spectrographs beyond the *Hubble Space Telescope*'s Cosmic Origins Spectrograph, which will have limited or no sensitivity in the wavelength region where the Feshbach resonances are expected. So a further, more sensitive, search for astrophysical H⁻ may be a long time coming.

This work was funded through NASA contract NAS5-32985. The research made use of the MAST *FUSE* archive. We would like to thank the referee for his comments; they have greatly improved the quality of the manuscript.

REFERENCES

- Andre, M. K., et al. 2002, BAAS, 34, 1179
 Bahng, J. 1969, MNRAS, 143, 73
 Balling, P., et al. 2000, Phys. Rev. A, 61, 022702
 Black, J. H. 1978, ApJ, 222, 125
 Broad, J. T., & Reinhardt, W. P. 1976, Phys. Rev. A, 14, 2159
 Bryant, H. C., et al. 1977, Phys. Rev. Lett., 38, 228
 Cohen, S., & Bryant, H. C. 2000, Rev. Mex. A&A, 9, 148
 Chandrasekhar, S. 1944, ApJ, 100, 176
 Chandrasekhar, S., & Breen, F. H. 1946, ApJ, 104, 430
 Chen, M.-K. 2002, European J. Phys. D, 21, 13
 Dalgarno, A., & McCray, R. A. 1973, ApJ, 181, 95
 Diplas, A., & Savage, B. D. 1994, ApJS, 93, 211
 Fano, U. 1961, Phys. Rev., 124, 1866
 Field, D. 2000, A&A, 362, 774
 Glover, S. C., Savin, D. W., & Jappson, A.-K. 2006, ApJ, 640, 553
 Jenkins, E. B., et al. 1973, ApJ, 181, L122
 Jensen, A. G., Rachford, B. L., & Snow, T. P. 2007, ApJ, 654, 955
 Lin, C. D. 1975, Phys. Rev. Lett., 35, 1150
 Lindroth, E. 1995, Phys. Rev. A, 52, 2737
 Macek, J. 1967, Proc. Phys. Soc. London, 92, 365
 McGowan, J. W., Williams, J. F., & Curley, E. K. 1969, Phys. Rev., 180, 132
 Mihalas, D. 1978, Stellar Atmospheres (2nd ed.; San Francisco: Freeman)
 Modeley, D., et al. 2003, J. Phys. B, 36, 4035
 Moos, H. W., et al. 2000, ApJ, 538, L1
 Münch, D. 1945, ApJ, 102, 385
 Rachford, B. L., et al. 2002, ApJ, 577, 221
 Rau, A. R. P. 1996, J. Astrophys. Astron., 17, 113
 Rawlings, J. M. C., Williams, D. A., & Canjo, J. 1988, MNRAS, 230, 695
 Rudkjøbing, M. 1969, Ap&SS, 3, 102
 Schild, R., Chaffee, F., Frogel, J. A., & Persson, S. E. 1974, ApJ, 190, 73
 Schmeltekopf, A. L., Fehsenfeld, F. C., & Ferguson, E. E. 1967, ApJ, 148, L155
 Snow, T. P. 1973, ApJ, 184, 135
 ———. 1975, ApJ, 198, 361
 Tang, J., et al. 1994, Phys. Rev. A, 49, 1021
 Taylor, A. J., & Burke, P. G. 1967, Proc. Phys. Soc. London, 92, 336
 Wildt, R. 1939, ApJ, 90, 611
 Wolf, N. J., Schwarzschild, M., & Rose, W. K. 1964, ApJ, 140, 833